

axes and thus on the offset between the nearest-neighbor chains along *b*. The energy curves (Figure 25) display minima both in Coulomb and in van der Waals terms for an offset similar to the observed arrangement. Thus the calculated degree of offset in the *bc* plane is completely compatible with that of the observed orthorhombic structure. We next examined ways of juxtaposing the (100) layers via symmetry elements, other than the observed, to yield different crystal structures. Space group *Pn11* was obtained by relating the (100) layers by translation along the *a* axis. Space group *P2₁/n11* was generated via a 2₁ axis relating the (100) layers. Space group *P112₁* was generated by replacing the *n* glide, forming the catemer chain, by a 2₁ axis.⁵³ This change is possible because the catemer chain is almost coplanar, and thus the *n* glide and the 2₁ axis yield almost the same contacts. All three alternative crystal structures were found to be appreciably less stable (by at least 5 kcal/mol) than the observed structure.

In summary, we have demonstrated for the two forms of oxalic acid and for formic acid that the observed crystal structure is more stable than an assortment of possible alternative packing arrangements, each incorporating the hydrogen-bonding motif of the observed structure.

(53) It is noteworthy that tetrolic acid,¹⁸ which appears in the catemer motif, crystallizes in space group *P2₁*.

9. Summary

Information contained in experimental electron density distributions was used to improve the electrostatic parameters of the carboxyl group and thus to obtain a better estimate of the Coulomb intermolecular energies in crystals of carboxylic acids.

By energy calculations using the improved parameters, we were able to account for various characteristic properties of molecular packing of carboxylic acids.

Acknowledgment. We thank Professor F. Hirshfeld for his advice and a critical reading of the manuscript. This research was supported by a grant from the United States-Israel Binational Science Foundation (BSF), Jerusalem, Israel.

Registry No. Fumaric acid, 110-17-8; oxalic acid, 144-62-7; formic acid, 64-18-6; terephthalic acid, 100-21-0; benzoic acid, 65-85-0; trimelic acid, 554-95-0; (*E,E*)-muconic acid, 3588-17-8; formamide, 75-12-7; tetrolic acid, 590-93-2; furan- α,α' -dicarboxylic acid, 3238-40-2; fumaric acid, 2987-87-3; methyl fumarate, 2756-87-8; methyl (*E,E*)-muconate, 10085-20-8; *p*-chlorobenzoic acid, 74-11-3; *p*-bromobenzoic acid, 586-76-5; *p*-nitrobenzoic acid, 62-23-7; 2-chlorobiphenyl-4-carboxylic acid, 5728-41-6; 2'-chlorobiphenyl-4-carboxylic acid, 3808-93-3; 2'-iodobiphenyl-4-carboxylic acid, 3808-95-5; *o*-fluorobenzoic acid, 445-29-4; *o*-chlorobenzoic acid, 118-91-2; *o*-bromobenzoic acid, 88-65-3; 1-naphthoic acid, 86-55-5; 2-naphthoic acid, 93-09-4.

Electronic Structures of Bent-Sandwich Compounds of the Main-Group Elements: A Molecular Orbital and UV Photoelectron Spectroscopic Study of Bis(cyclopentadienyl)tin and Related Compounds

S. G. Baxter,^{1a} A. H. Cowley,^{*1a} J. G. Lasch,^{1a} M. Lattman,^{*1b} W. P. Sharum,^{1b} and C. A. Stewart^{1a}

Contribution from the Departments of Chemistry, The University of Texas at Austin, Austin, Texas 78712, and Southern Methodist University, Dallas, Texas 75275. Received July 27, 1981

Abstract: An SCF $X\alpha$ scattered-wave ($X\alpha$ -SW) calculation has been performed on the bent-sandwich molecule (η^5 -C₅H₅)₂Sn (stannocene). The $X\alpha$ -SW calculation revealed that the highest occupied MO's (6a₂ and 9b₂) are π type and highly localized on the cyclopentadienyl rings. In order of decreasing energy, the MO's associated with the bonding of the C₅H₅ group to Sn are 11a₁, 6b₁, 10a₁, 8b₂, and 9a₁. Of these MO's, the one exhibiting the largest tin lone pair character is 10a₁. The MO's 5a₂, 5b₁, and 8a₁ to 2b₂ inclusive are σ_{CC} and σ_{CH} in character, highly localized on the C₅H₅ rings, and comparable in energy to the corresponding MO's of ferrocene. An MNDO calculation on (C₅H₅)₂Si and the isoelectronic species [(C₅H₅)₂P]⁺ indicated that a bis(pentahapto) structure is the global minimum in both cases. The sequences of the higher MO's of (η^5 -C₅H₅)₂Si and (η^5 -C₅H₅)₂Sn as computed by the MNDO and $X\alpha$ -SW methods, respectively, are in good mutual agreement. He(I) ultraviolet spectra (UV PES) have been measured for (η^5 -C₅H₅)₂Sn, (η^5 -C₅H₅)₂Pb, (η^5 -Me₅C₅)₂Sn, and (η^5 -Me₅C₅)₂Pb. The UV PES data have been interpreted with the aid of theoretical ionization energies computed for (η^5 -C₅H₅)₂Sn by the transition-state method. The synthesis of (η^5 -Me₅C₅)₂Pb is described.

The electronic structures and patterns of stability of the π complexes of the transition and f-block elements are now understood reasonably well. By contrast, much less is known about compounds that feature multihapto bonding between the main-group elements and carbocyclic ligands. Some progress has been made toward understanding π -bonded cyclopentadienyl compounds of the group 1A and 2A elements such as (η^5 -C₅H₅)Li² and (η^5 -C₅H₅)BeX³ and the intriguing molecule beryllocene,

(C₅H₅)₂Be.⁴ However, our understanding of the bent-sandwich molecules of the group 4A elements is much less complete and, in fact, molecular orbital (MO) calculations on such systems are confined to one semiempirical MO study of stannocene, (η^5 -C₅H₅)₂Sn.⁵ The present paper represents an attempt to develop a theoretical model for bent-sandwich molecules. We were particularly interested in the nature of the bonding between the

(1) (a) University of Texas at Austin. (b) Southern Methodist University.
 (2) (a) Janoschek, R.; Diercksen, G.; Preuss, H. *Int. J. Quantum Chem. Symp.* **1967**, *1*, 205-208. (b) Alexandratos, S.; Streitwieser, A., Jr.; Schaefer, H. F., III *J. Am. Chem. Soc.* **1976**, *98*, 7959-7962.
 (3) (a) Dewar, M. J. S.; Rzepa, H. S. *J. Am. Chem. Soc.* **1978**, *100*, 777-784. (b) Jemmis, E. D.; Alexandratos, S.; Schleyer, P. v. R.; Streitwieser, A., Jr.; Schaefer, H. F., III, *J. Am. Chem. Soc.* **1978**, *100*, 5695-5700. (c) Böhm, M. C.; Gleiter, R.; Morgan, G. L.; Luszyk, J.; Starowieyski, K. B. *J. Organomet. Chem.* **1980**, *194*, 257-263. (d) Marynick, D. S. *J. Am. Chem. Soc.* **1981**, *103*, 1328-1333.

(4) Most, but not all, MO calculations on beryllocene favor an η^5 - η^1 ground-state structure. For pertinent references see: (a) Sundbom, M. *Acta Chem. Scand.* **1966**, *20*, 1608-1620. (b) Lopatko, O. Y.; Klimentko, N. M.; Dyatkina, M. E. *Zh. Strukt. Khim.* **1972**, *13*, 1128-1133. (c) Marynick, D. S. *J. Am. Chem. Soc.* **1977**, *99*, 1436-1441. (d) Chiu, N.-S.; Schäfer, L. *Ibid.* **1978**, *100*, 2604-2607. (e) Demuyck, J.; Rohmer, M. M. *Chem. Phys. Lett.* **1978**, *54*, 567-570. (f) Gleiter, R.; Böhm, M. C.; Haaland, A.; Johansen, R.; Luszyk, J. *J. Organomet. Chem.* **1979**, *170*, 285-292 and ref 2a and 2b.
 (5) Jutzki, P.; Kohl, F.; Hofmann, P.; Krüger, C.; Tsay, Y.-H. *Chem. Ber.* **1980**, *113*, 757-769.

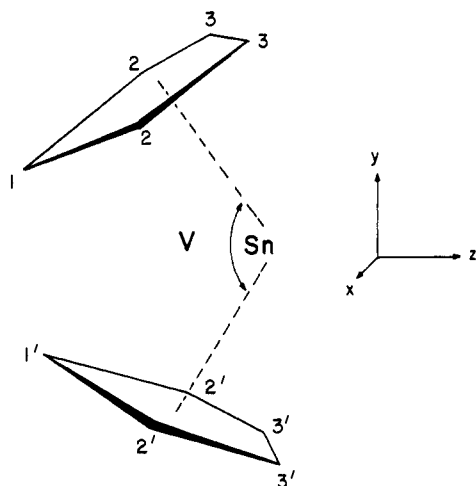


Figure 1. The geometry of $(\eta^5\text{-C}_5\text{H}_5)_2\text{Sn}$ (omitting the hydrogen atoms). $V = 146^\circ$, $d_{\text{SnC}} = 2.70 \text{ \AA}$, $d_{\text{CC}} = 1.42 \text{ \AA}$, $d_{\text{CH}} = 1.14 \text{ \AA}$. The molecule has C_{2v} symmetry and the equivalent carbon atoms have identical numbers; unprimed and primed numbers indicate different rings. The Sn, C₁, and C_{1'} atoms lie in the yz plane.

cyclopentadienyl rings and the group 4A element, the composition of the HOMO, and the identification of MO's possessing lone pair character. The approach taken is a hybrid one and involves the use of experimental ultraviolet photoelectron spectroscopic (UV PES) data for $(\eta^5\text{-C}_5\text{H}_5)_2\text{M}^6$ and their permethylated analogues, $(\eta^5\text{-Me}_5\text{C}_5)_2\text{M}$ ($\text{M} = \text{Sn}, \text{Pb}$), and SCF $X\alpha$ scattered-wave ($X\alpha\text{-SW}$) calculations on $(\eta^5\text{-C}_5\text{H}_5)_2\text{Sn}$. The $X\alpha\text{-SW}$ method⁷ is well suited to the interpretation of photoelectron spectroscopic data, when used in conjunction with transition-state calculations,⁸ which circumvent the use of Koopmans' theorem.⁹ Stannocene was chosen for the $X\alpha\text{-SW}$ study because it is the only monomeric bis(cyclopentadienyl) compound of a group 4A element with an accurately known structure.¹⁰ Finally, to broaden the scope of the study we have performed MNDO calculations¹² on the iso-electronic systems $(\text{C}_5\text{H}_5)_2\text{Si}$ and $[(\text{C}_5\text{H}_5)_2\text{P}]^+$.

Theoretical Methods

The $X\alpha\text{-SW}$ calculations on $(\eta^5\text{-C}_5\text{H}_5)_2\text{Sn}$ were made by employing the spin-restricted procedure of Johnson and Slater.⁷ The requisite bond distances and angles for $(\eta^5\text{-C}_5\text{H}_5)_2\text{Sn}$ were based on our recent single-crystal X-ray diffraction determination.¹¹ The solid state of $(\eta^5\text{-C}_5\text{H}_5)_2\text{Sn}$ comprises two distinct types of molecules which differ primarily in the ring centroid-tin-ring centroid angles, V (148.0° in molecule I and 143.7° in molecule II). For

(6) He(I) UV PES data have been reported previously for $(\text{C}_5\text{H}_5)_2\text{Sn}$ and $(\text{C}_5\text{H}_5)_2\text{Pb}$. See: Craddock, S.; Duncan, W. *J. Chem. Soc., Faraday Trans. 2* **1978**, *74*, 194–202. There is reasonable agreement between the present and previous results.

(7) (a) Slater, J. C. *Adv. Quantum Chem.* **1972**, *6*, 1. (b) Johnson, K. H. *Ibid.* **1973**, *7*, 143–185. (c) Johnson, K. H. *Annu. Rev. Phys. Chem.* **1975**, *26*, 39–57.

(8) (a) Slater, J. C.; Johnson, K. H. *Phys. Rev. B* **1972**, *5*, 844–853. (b) Slater, J. C. "Quantum Theory of Molecules and Solids"; McGraw-Hill: New York, 1974; Vol. 4, p 583.

(9) Koopmans, T. *Physica (Utrecht)* **1934**, *1*, 104–113.

(10) The X-ray crystal structure of $(\text{C}_5\text{H}_5)_2\text{Sn}$ has been determined recently¹¹ and this molecule has been found to be monomeric in the solid state. By contrast the solid-state structure of the lead analogue, $(\text{C}_5\text{H}_5)_2\text{Pb}$, consists of a zigzag polymeric structure with alternating bridging and terminal cyclopentadienyl groups (Panattoni, C.; Bombieri, G.; Croatto, U. *Acta Crystallogr.* **1966**, *21*, 823–826). Both $(\text{C}_5\text{H}_5)_2\text{Sn}$ and $(\text{C}_5\text{H}_5)_2\text{Pb}$ are monomeric in the vapor phase by electron diffraction. However, the ring centroid-metal-ring centroid angles were not determined sufficiently accurately for our purposes. See: Almenningen, A.; Haaland, A.; Motzfeldt, T. *J. Organomet. Chem.* **1967**, *7*, 97–104. Bis(cyclopentadienyl)germanium has been prepared; however, it is rather unstable and has not yet been characterized structurally. See: Scibelli, J. V.; Curtis, M. D. *J. Am. Chem. Soc.* **1973**, *95*, 924–925.

(11) Atwood, J. L.; Hunter, W. E.; Cowley, A. H.; Jones, R. A.; Stewart, C. A. *J. Chem. Soc., Chem. Commun.* **1981**, 925.

(12) Dewar, M. J. S.; McKee, M. L.; Rzepa, H. S. *J. Am. Chem. Soc.* **1978**, *100*, 3607 and references therein.

Table I. $X\alpha\text{-SW}$ "Ground-State" Eigenvalues and Charge Densities^a for $(\eta^5\text{-C}_5\text{H}_5)_2\text{Sn}$

MO	ϵ^b	Sn				C		H	out-	in-
		s	p	d	f	s	p	s	er ^c	ter ^d
12a ₁	-1.32	0.03	0.29	0.01	0.01	0.00	0.22	0.00	0.03	0.41
7b ₁	-1.41		0.32	0.01	0.01	0.00	0.24	0.00	0.01	0.41
6a ₂	-4.26			0.04	0.00	0.00	0.72	0.00	0.00	0.24
9b ₂	-4.27		0.01	0.04	0.01	0.00	0.70	0.00	0.01	0.23
11a ₁	-4.93	0.07	0.11	0.03	0.00	0.00	0.54	0.00	0.00	0.25
6b ₁	-5.33		0.25	0.00	0.01	0.00	0.54	0.00	0.01	0.20
10a ₁	-6.25	0.25	0.12	0.01	0.00	0.00	0.42	0.00	0.00	0.20
8b ₂	-8.89		0.14	0.00	0.00	0.00	0.64	0.00	0.01	0.21
5a ₂	-10.77			0.00	0.00	0.04	0.68	0.28	0.00	0.00
5b ₁	-10.78		0.00	0.00	0.00	0.00	0.68	0.28	0.00	0.04
9a ₁	-10.82	0.53	0.00	0.00	0.00	0.00	0.30	0.00	0.00	0.17
8a ₁	-10.84	0.00	0.00	0.00	0.00	0.02	0.72	0.26	0.00	0.00
7b ₂	-10.84		0.00	0.00	0.00	0.02	0.68	0.26	0.00	0.04
6b ₂	-11.34		0.00	0.00	0.00	0.00	0.64	0.36	0.00	0.00
4a ₂	-11.35			0.00	0.00	0.00	0.62	0.36	0.01	0.01
7a ₁	-11.37	0.00	0.00	0.00	0.00	0.00	0.64	0.36	0.00	0.00
4b ₁	-11.38		0.00	0.00	0.00	0.00	0.62	0.36	0.00	0.02
5b ₂	-14.54		0.00	0.00	0.00	0.04	0.54	0.38	0.01	0.03
6a ₁	-14.57	0.00	0.00	0.00	0.00	0.04	0.54	0.42	0.00	0.00
3a ₂	-15.03			0.00	0.00	0.28	0.54	0.16	0.00	0.02
3b ₁	-15.04		0.00	0.00	0.00	0.28	0.54	0.16	0.00	0.02
4b ₂	-15.11		0.00	0.00	0.00	0.30	0.46	0.22	0.00	0.02
5a ₁	-15.13	0.00	0.00	0.00	0.00	0.30	0.48	0.22	0.00	0.00
2a ₂	-19.25			0.01	0.00	0.68	0.16	0.12	0.00	0.02
3b ₂	-19.25		0.00	0.00	0.00	0.68	0.20	0.08	0.00	0.04
4a ₁	-19.28	0.00	0.00	0.00	0.00	0.68	0.20	0.08	0.00	0.04
2b ₁	-19.29		0.00	0.00	0.00	0.68	0.16	0.12	0.00	0.04
3a ₁	-24.45	0.01	0.00	0.02	0.00	0.76	0.20	0.00	0.00	0.01
2b ₂	-24.45		0.01	0.01	0.00	0.76	0.20	0.00	0.00	0.02
2a ₁	-26.93	0.00	0.00	1.00	0.00	0.00	0.00	0.00	0.00	0.00
1a ₂	-26.93			1.00	0.00	0.00	0.00	0.00	0.00	0.00
1b ₁	-26.93		0.00	1.00	0.00	0.00	0.00	0.00	0.00	0.00
1b ₂	-26.95		0.00	0.99	0.00	0.00	0.00	0.00	0.00	0.01
1a ₁	-26.98	0.00	0.00	0.98	0.00	0.00	0.00	0.00	0.00	0.02

^a Charge densities are the percentage of electron densities within the atomic spheres. ^b Eigenvalues in eV. ^c Charge density outside outer sphere. ^d Intersphere charge density inside outer sphere and not accounted for by atomic spheres. The dashed line denotes the HOMO/LUMO separation.

the purpose of the present calculations, averages of the metric parameters for molecules I and II were employed and are illustrated in Figure 1. The atomic sphere radii could not be chosen on the basis of optimizing the virial ratio¹³ because of the large Sn–C distances. Therefore, from the initial $X\alpha$ charge distribution derived from the superposition of free atom charge densities, a ratio of radii was selected from the values of the radius of each atom which just enclosed the number of electrons assigned from atomic structures.¹³ The absolute radii were chosen at a point where the carbon and tin spheres were tangential, while the carbon and hydrogen spheres were overlapping. The radii obtained in this manner were $r_{\text{Sn}} = 3.219$, $r_{\text{C}} = 1.858$, and $r_{\text{H}} = 1.475$ au. The outer-sphere radius was chosen to be tangential to the outermost hydrogen sphere, $r_{\text{outer}} = 7.820$ au. Schwartz's exchange parameter,¹⁴ α_{HF} , was used for carbon, and Slater's value¹⁵ was employed for hydrogen. The α value for tin, 0.701, was estimated by extrapolation of Schwartz's values.¹⁴ α_{outer} was taken to be equal to α_{H} , while the intersphere exchange parameter, α_{int} , was calculated to be 0.758 on the basis of averaging the atomic α values according to the number of valence electrons. Spherical harmonics through $l = 3$ were employed for the tin and outer spheres, while values through $l = 1$ and 0 were used for carbon and hydrogen, respectively. All SCF calculations converged to better than 0.01 eV while keeping all cores (except the Sn(4d)) fixed. The first

(13) (a) Norman, J. G. *J. Chem. Phys.* **1974**, *61*, 4630–4635. (b) Norman, J. G. *Mol. Phys.* **1976**, *31*, 1191–1198.

(14) Schwartz, K. *Phys. Rev. B: Condens. Matter.* **1972**, *5*, 2466–2468.

(15) Slater, J. C. *Int. J. Quantum Chem. Symp.* **1973**, *7*, 533–544.

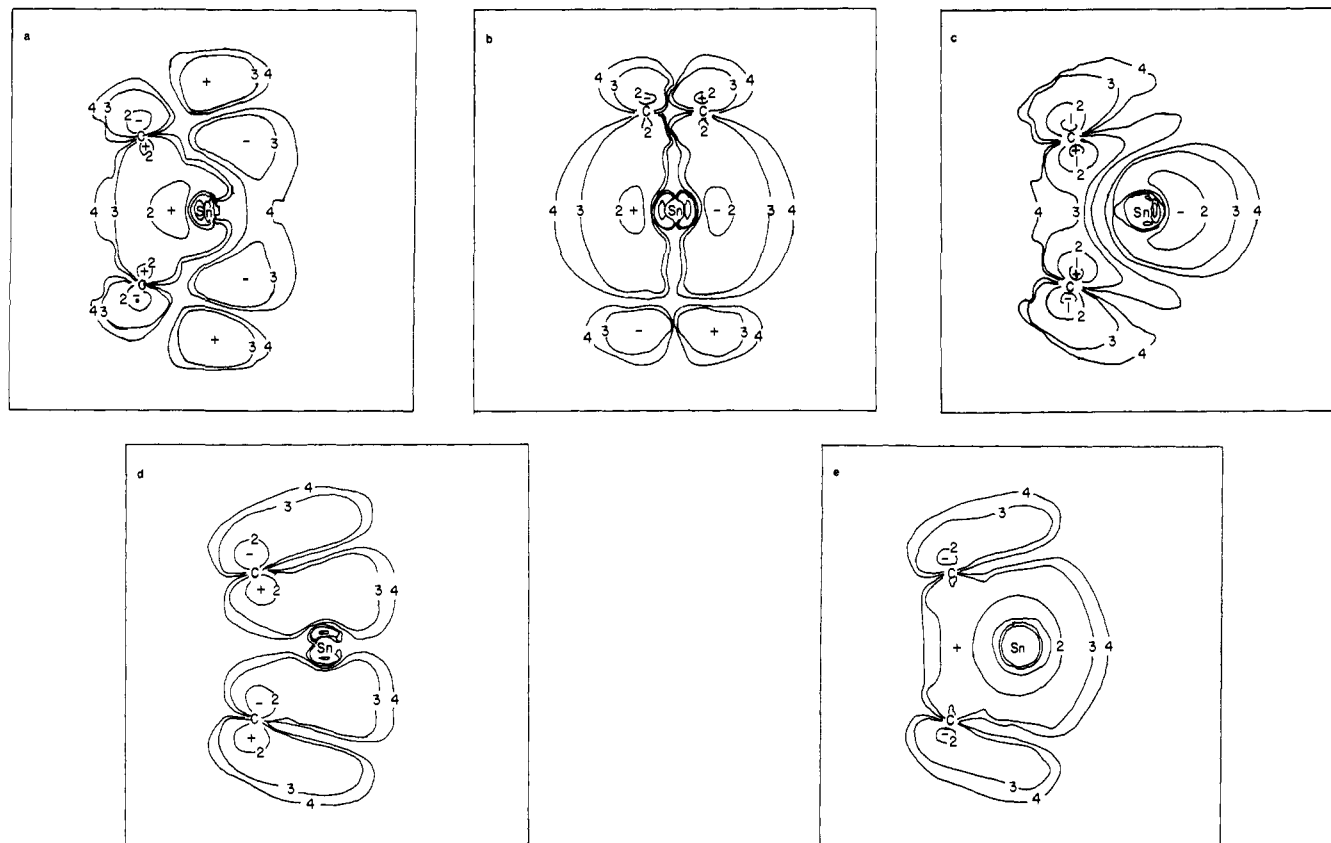


Figure 2. X α -SW contour plots for some MO's of (η^5 -C₅H₅)₂Sn: (a) 11a₁ (yz plane); (b) 6b₁ (plane containing Sn and both C₃ atoms); (c) 10a₁ (yz plane); (d) 8b₂ (yz plane); (e) 9a₁ (yz plane). Contour values: 1 = ± 0.13 ; 2 = ± 0.07 ; 3 = ± 0.02 ; 4 = ± 0.01 .

11 ionization energies (IE's) were computed by means of the transition-state method.⁸

Experimental Section

Materials. Bis(cyclopentadienyl)tin,^{16,17} (η^5 -C₅H₅)₂Pb,^{17,18} and (η^5 -Me₅C₅)₂Sn⁵ were prepared and purified according to literature methods.

Preparation of (Me₅C₅)₂Pb. Anhydrous PbCl₂ (2.60 g, 9.3 mmol) was added slowly via a solid addition funnel to a solution of 18.6 mmol of Me₅C₅Li in 45 mL of tetrahydrofuran under a dry nitrogen atmosphere. Filtration of the reaction mixture afforded a deep red solution, vacuum evaporation of which resulted in deep-red solid (Me₅C₅)₂Pb (mp 100–105 °C). The compound can be purified by sublimation in vacuo. ¹H NMR (90.0 MHz) δ 2.05 (s); ¹³C[¹H] (20.0 MHz) (Me₄Si) 9.7 (s, Me₅C₅), 117.6 (s, Me₅C₅). Anal. Calcd for C₂₀H₃₀Pb: C, 50.29; H, 6.34. Found: C, 48.32; H, 6.42. Even though the carbon analysis is low, the identity of the compound has been established unequivocally by single-crystal X-ray diffraction.¹¹

Spectroscopic Measurements. All UV PES measurements were made on a Perkin-Elmer Model PS-18 spectrometer with a He(I) source (21.22 eV). The samples were introduced via a direct inlet heated probe system at temperatures between 45 and 105 °C. A mixture of argon (15.759 eV) and xenon (12.130 eV) was used for the internal calibration of each spectrum. The resolution of the instrument was maintained at 25–50 meV and the temperature was controlled to ± 2 °C. All quoted IE's are band maxima unless otherwise indicated.

Results and Discussion

The Molecular Orbitals of Stannocene. The two highest filled MO's of stannocene (6a₂ and 9b₂) differ in energy by only 0.01 eV (Table I). Both orbitals are highly localized on the cyclopentadienyl groups and can be viewed as arising from the e₁'/ π -type MO's for a pair of parallel C₅H₅ rings in D_{5h} symmetry. Tin 5p and 5s atomic orbital participation in the 6a₂ MO of stannocene is, of course, precluded in C_{2v} symmetry, hence this MO exhibits only a very minimal Sn(4d) contribution. The 9b₂ MO features very small Sn(5p) and Sn(4d) participation. The

MO's associated with the strongest bonding of the π -cyclopentadienyl electrons to tin are 11a₁, 6b₁, 10a₁, 8b₂, and 9a₁. The 11a₁ MO is the least strong ring–tin bonding MO. The contour diagram in Figure 2a and the charge density data (Table I) indicate that the primary interaction occurs between the ring π MO's and the Sn(5p_z) AO. There is, however, also significant participation of the Sn(5s) AO in this MO. Somewhat stronger ring–tin interaction is evident in the 6b₁ MO. The fact that this orbital involves a very substantial amount of Sn(5p_z) character is apparent from a contour diagram drawn in a plane including Sn and the two ring C₃ atoms (Figure 2b). It is quite clear from Figure 2c that the 10a₁ MO is the stannocene "lone pair". As in other X α -SW calculations,¹⁹ vestigial lone pair character can be found in other orbitals of the same symmetry, such as 9a₁ and 11a₁. Also, note the presence of a small bonding interaction in the left-hand side of the 10a₁ contour diagram. As expected, the strongest bonding between the cyclopentadienyl rings and a tin 5p orbital occurs in the 8b₂ MO when both lobes of the latter are pointing toward the ligands (Figure 2d). The lowest energy MO involved in Sn–ring bonding is 9a₁. This orbital, which is illustrated in Figure 2e, arises solely from interaction of the Sn(5s) orbital with an a₁ combination of ring π MO's.

The MO's 5a₂, 5b₁, and 8a₁ to 2b₂ inclusive are σ -bonding levels which are highly localized on the cyclopentadienyl rings. As shown in Figure 3, there is relatively little perturbation of these σ_{CC} and σ_{CH} MO's on proceeding from ferrocene to stannocene. Making due allowances for the symmetry difference, the corresponding levels have been connected by dashed lines. Finally, the five lowest occupied MO's, viz., 2a₁, 1a₂, 1b₁, 1b₂, and 1a₁, are filled tin 4d_{x²-y²}, 4d_{xy}, 4d_{xz}, 4d_{yz}, and 4d_{z²}, respectively. Since these orbitals are very closely spaced it seems doubtful whether the effects of the ligand field would be discernible.²⁰

(19) See, for example: Cowley, A. H.; Lattman, M.; Walker, M. L. *J. Am. Chem. Soc.* **1979**, *101*, 4074–4080.

(20) Ligand field splitting effects have been detected in the UV PES of some simple d¹⁰ dialkyls. See, for example: Bancroft, G. M.; Creber, D. K.; Basch, H. *J. Chem. Phys.* **1977**, *67*, 4891–4897.

(16) Fischer, E. O.; Grubert, H. *Z. Naturforsch.*, **B** **1956**, *11B*, 423–424.
(17) Dave, L. D.; Evans, D. F.; Wilkinson, G. *J. Chem. Soc.* **1959**, 3684–3688.

(18) Fischer, E. O.; Grubert, H. *Z. Anorg. Chem.* **1956**, *286*, 237–242.

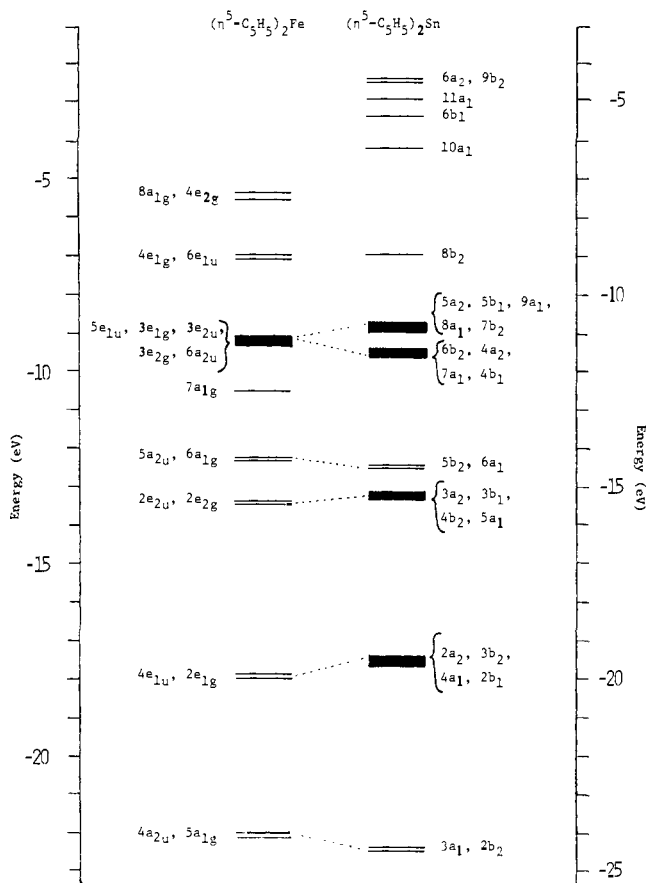


Figure 3. Comparison of the energies of the occupied MO's of $(\eta^5\text{-C}_5\text{H}_5)_2\text{Fe}$ and $(\eta^5\text{-C}_5\text{H}_5)_2\text{Sn}$ as computed by the X α -SW method. (The data for $(\eta^5\text{-C}_5\text{H}_5)_2\text{Fe}$ are taken from Rösch and Johnson.²⁹)

Table II. MNDO Computed Energies for Various $(\text{C}_5\text{H}_5)_2\text{Si}$ Structures and a Comparison of Higher MO Energies for $(\eta^5\text{-C}_5\text{H}_5)_2\text{Sn}$ and $(\eta^5\text{-C}_5\text{H}_5)_2\text{Si}$

$(\text{C}_5\text{H}_5)_2\text{Si}$ structure	ΔH_f , kcal/mol	rel energy, kcal/mol
bis(pentahapto) (D_{5h}) (1) ^a	50.76	0.00
bis(pentahapto) (C_{2v}) (2)	59.19	8.43
bis(monohapto) (a)(a) ^b	72.98	22.22
bis(monohapto) (+)(+) ^b	74.27	23.51
bis(monohapto) (+)(-) ^b	77.46	26.70

MO ^c	energy, eV		description
	$(\eta^5\text{-C}_5\text{H}_5)_2\text{Sn}$	$(\eta^5\text{-C}_5\text{H}_5)_2\text{Si}$ ^d	
6a ₂	-4.26	-8.54	ring π
9b ₂	-4.27	-8.55	ring π
11a ₁	-4.93	-9.46	heteroatom lone pair
6b ₁	-5.33	-10.09	Cp ring-heteroatom np_x
10a ₁	-6.25	-10.69	heteroatom lone pair

^a There is virtually no difference in energy between the eclipsed (D_{5h}) and staggered (D_{5d}) structures. ^b The symbols in parentheses reflect the relative orientations of the $\eta^5\text{-C}_5\text{H}_5$ rings about the silicon-carbon bond. See 3, 4, and 5 in text. ^c The X α -SW orbital labeling scheme has been employed to facilitate comparison of the MO's of $(\eta^5\text{-C}_5\text{H}_5)_2\text{Sn}$ and $(\eta^5\text{-C}_5\text{H}_5)_2\text{Si}$, even though d orbitals were not included in the basis set of Si. ^d These eigenvalues refer to structure 2 with $V = 145^\circ$. See text.

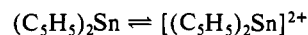
Apart from some differences in labeling, the foregoing sequence for the higher occupied MO's of stannocene is qualitatively similar to that arrived at by Jutzi et al.⁵ with semiempirical calculations. The major difference in the results is that Jutzi et al.⁵ computed the HOMO to be the tin lone pair orbital (10a₁ MO in the present paper). As noted above, the X α -SW calculation indicates that the tin lone pair character is concentrated in the fifth occupied MO. This MO is ~ 2 eV more stable than the highest occupied

Table III. Computed Ionization Energies for $(\eta^5\text{-C}_5\text{H}_5)_2\text{Sn}$ and Experimental Ionization Energies for $(\eta^5\text{-C}_5\text{H}_5)_2\text{Sn}$, $(\eta^5\text{-C}_5\text{H}_5)_2\text{Pb}$, $(\eta^5\text{-Me}_5\text{C}_5)_2\text{Sn}$, and $(\eta^5\text{-Me}_5\text{C}_5)_2\text{Pb}$

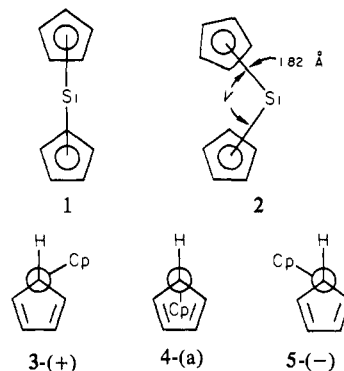
MO ^a	computed IE, eV ^d	experimental IE's, eV			
		$(\eta^5\text{-C}_5\text{H}_5)_2\text{Sn}$	$(\eta^5\text{-C}_5\text{H}_5)_2\text{Pb}$	$(\eta^5\text{-Me}_5\text{C}_5)_2\text{Sn}$	$(\eta^5\text{-Me}_5\text{C}_5)_2\text{Pb}$
6a ₂	6.60	7.57	7.55	6.60	6.33
9b ₂	6.61	7.91	7.85	6.60	6.88
11a ₁	7.31	8.85	8.54	7.64	7.38
6b ₁	7.64	8.85	8.88	7.64	7.38
10a ₁	8.74	9.58	10.10	8.40	8.93
8b ₂	11.25	10.5	10.6	9.4	9.38
5a ₂	13.34				
5b ₁	13.35	11.2	12.0	10.2	10.0
9a ₁	13.41	to	to	to	to
8a ₁	13.46	14.0	14.5	16.0	16.0
7b ₂	13.41				

^a The orbital labeling employed is that of the X α -SW calculation on $(\eta^5\text{-C}_5\text{H}_5)_2\text{Sn}$ and it has been used for the other compounds.

MO's, which are two very closely spaced ring-localized π MO's. As will be shown later, the X α -SW calculation is also consistent with the experimental UV PES data. Moreover, the X α -SW sequence of MO's explains why cyclic voltammetric experiments on stannocene²¹ result in an irreversible oxidation wave rather than the process



MNDO Calculations on $(\text{C}_5\text{H}_5)_2\text{Si}$. As a further check on the position of the lone pair MO, we have performed MO calculations on the related molecule $(\text{C}_5\text{H}_5)_2\text{Si}$. (This species was chosen because MNDO parameters are only available up to chlorine.) A geometry search for the as yet unknown compound, $(\text{C}_5\text{H}_5)_2\text{Si}$, revealed that the bis(pentahapto) structure, **1**, is the global minimum and is favored by >20 kcal/mol (Table II) over any of the monohapto structures (which differ in orientation of the C_5H_5 ring along the C-Si axis, see 3-5). Note that the MNDO calculation predicts a D_{5h} sandwich structure, **1**, rather than the expected C_{2v} structure, **2**. Two comments are in order on this



point. First, the potential for distortion of **1** toward **2** is rather "soft" and the energy difference between structures with $V = 180^\circ$ and 145° is only 8.4 kcal/mol. Second, we have encountered a rather similar situation in the case of SF_4 for which the MNDO geometry-optimized structure was of T_d symmetry rather than the expected C_{2v} arrangement.¹⁹ To facilitate comparisons between the MO's of $(\eta^5\text{-C}_5\text{H}_5)_2\text{Si}$ and $(\eta^5\text{-C}_5\text{H}_5)_2\text{Sn}$, an MNDO computation was carried out on the former with the ring centroid-silicon-ring centroid angle, V , fixed at 145° . The MO's arrived at in this manner are presented in Table II. As in the X α -SW calculation on $(\eta^5\text{-C}_5\text{H}_5)_2\text{Sn}$, the first two occupied MO's of $(\eta^5\text{-C}_5\text{H}_5)_2\text{Si}$ are localized in the cyclopentadienyl rings and rather close together in energy. In fact, both the sequences and energy differences of, e.g., the first five occupied MO's for the X α -SW and MNDO calculations are in very satisfactory agreement as

(21) Cowley, A. H.; Mills, J. L., unpublished observation.

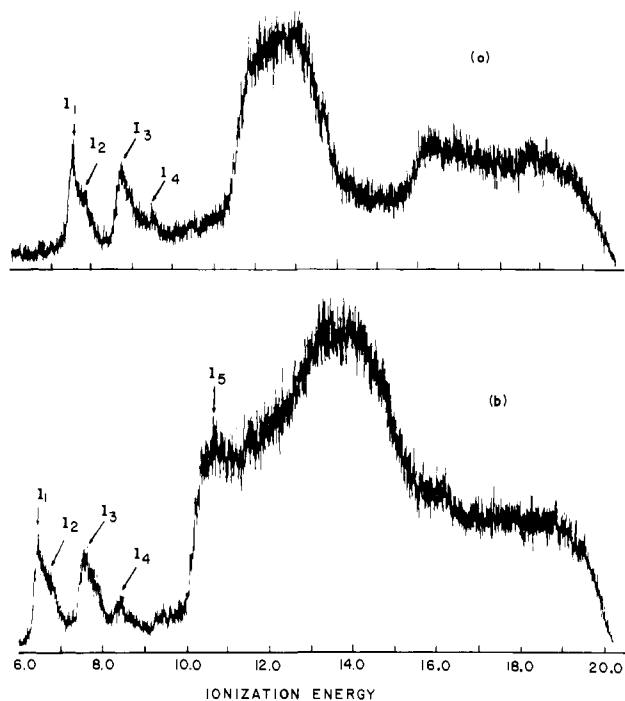


Figure 4. He(I) UV PES of (a) $(\eta^5\text{-C}_5\text{H}_5)_2\text{Sn}$ and (b) $(\eta^5\text{-Me}_5\text{C}_5)_2\text{Sn}$.

shown in Table II. The MNDO calculation on $(\eta^5\text{-C}_5\text{H}_5)_2\text{Si}$ indicates that the silicon lone pair is distributed among the third ($11a_1$) and fifth ($10a_1$) MO's.

Interpretation of the UV Photoelectron Spectra of $(\eta^5\text{-C}_5\text{H}_5)_2\text{Sn}$ and Related Compounds. Transition-state calculations have been carried out for the first 11 ionizations of stannocene and the computed IE's are assembled in Table III. As is usually found for main-group systems,²² the sequence of computed IE's is the same as that of the ground-state MO's.

Use of the transition-state computed IE's permits ready interpretation of the UV PES of stannocene (Figure 4). Thus, the first sharp peak at 7.57 eV (I_1) and its associated shoulder at 7.91 eV (I_2) are attributed to electron ejection from the cyclopentadienyl ring localized MO's $6a_2$ and $9b_2$, respectively. The broader peak (I_3) at 8.85 eV is of approximately equal intensity to the first, thus suggesting that it involves two ionizations, namely from the $11a_1$ and $6b_1$ ring-tin bonding MO's. I_4 , the lower intensity peak at 9.58 eV, is attributed to electron ejection from the $10a_1$ MO which is the stannocene lone pair orbital. Electron ejection from the $8b_2$ MO is responsible for the barely detectable feature at 10.5 eV. This ionization is somewhat more discernible in the He(II) spectra of all four bent-sandwich molecules. Ionization from the $9a_1$ MO contributes to the broad, intense envelope between 11.2 and 14.0 eV. An alternative assignment would attribute peak I_1 to electron ejection from the $6a_2$ and $9b_2$ MO's, peak I_2 to electron ejection from the $11a_1$ MO, and peaks I_3 and I_4 to electron ejection from the $6b_1$ and $10a_1$ MO's, respectively. However, since this assignment produces a less satisfactory agreement with the experimental peak intensities we consider it much less likely.

The UV PES of the other three compounds, $(\eta^5\text{-Me}_5\text{C}_5)_2\text{Sn}$ (Figure 4), $(\eta^5\text{-C}_5\text{H}_5)_2\text{Pb}$, and $(\eta^5\text{-Me}_5\text{C}_5)_2\text{Pb}$, can be interpreted in an analogous fashion and the assignments are indicated in Table III. Both $(\eta^5\text{-Me}_5\text{C}_5)_2\text{Sn}$ and $(\eta^5\text{-Me}_5\text{C}_5)_2\text{Pb}$ exhibit an additional spectral band at 10.75–10.80 eV that is peculiar to the permethylated compounds.²³ It seems reasonable to suggest that

(22) This is true unless the eigenvalues are very closely spaced. For representative examples, see: ref 19 for (SF_4) , Head et al. (Head, J. D.; Mitchell, K. A. R.; Noodleman, L.; Paddock, N. L. *Can. J. Chem.* 1977, 55, 669–681) for (P_4S_3) , Noodleman and Mitchell (Noodleman, L.; Mitchell, K. A. R. *Inorg. Chem.* 1978, 17, 2709–2717) for SO_2 and SO_2F_2 , and Noodleman and Paddock (Noodleman, L.; Paddock, N. L. *Inorg. Chem.* 1979, 18, 254–260) for Me_3N , $(\text{SiH}_3)_3\text{N}$, and $(\text{GeH}_3)_3\text{N}$.

Table IV. MNDO Computed Energies for Various $[(\text{C}_5\text{H}_5)_2\text{P}]^+$ Structures and the Higher MO Energies for $\text{C}_{2v} [(\eta^5\text{-C}_5\text{H}_5)_2\text{P}]^+$

[(C ₅ H ₅) ₂ P] ⁺ structure	ΔH_f , kcal/mol	rel energy, kcal/mol	C _{2v} [(η ⁵ -C ₅ H ₅) ₂ P] ⁺ energy, eV		description
			MO ^a		
bis(pentahapto) (C _{2v})	281.09	0	6a ₂	-12.97	ring π
bis(pentahapto) (D _{5h}) ^b	329.08	47.99	9b ₂	-14.27	Cp ring-P (3p _y)
bis(monohapto) (a)(a)	300.21	19.12	6b ₁	-14.90	Cp ring-P (3p _x)
bis(monohapto) (+)(+)	305.18	24.09	11a ₁	-15.29	P lone pair
bis(monohapto) (+)(-)	305.51	24.42	10a ₁	-15.88	P lone pair

^a The stannocene Xα-SW orbital labeling scheme has been used to facilitate comparison of the MO's of $(\eta^5\text{-C}_5\text{H}_5)_2\text{Si}$ and $(\eta^5\text{-C}_5\text{H}_5)_2\text{Sn}$, even though P(3d) orbitals were not included in the basis set. ^b There is virtually no difference in energy between the eclipsed (D_{5h}) and staggered (D_{5d}) structures.

this ionization is associated with the ring methyl groups.

The foregoing assignments are consistent with the electronic structural model discussed earlier. Note that the averages of the IE's for the $6a_2$ and $9b_2$ MO's are virtually identical for $(\eta^5\text{-C}_5\text{H}_5)_2\text{Sn}$ and $(\eta^5\text{-C}_5\text{H}_5)_2\text{Pb}$ and for $(\eta^5\text{-Me}_5\text{C}_5)_2\text{Sn}$ and $(\eta^5\text{-Me}_5\text{C}_5)_2\text{Pb}$. The fact that these ionizations are independent of the central atom is in accord with the view that the highest occupied MO's are ring localized and do not involve the heteroatom lone pairs. Another feature worthy of comment is the fact that the IE's pertaining to electron ejection from the central atom lone pair MO's are larger for $(\eta^5\text{-C}_5\text{H}_5)_2\text{Pb}$ and $(\eta^5\text{-Me}_5\text{C}_5)_2\text{Pb}$ than for the tin analogues. We attribute this observation to the fact that the ring centroid-metal-ring centroid angles are larger for the lead than for the tin compounds,²⁴ thus implying that the lead lone pairs involve more valence s character than the corresponding tin lone pairs.

Other Bent-Sandwich Systems. The 14 Interstitial Electron Rule.

From the foregoing Xα-SW and MNDO calculations on $(\eta^5\text{-C}_5\text{H}_5)_2\text{Sn}$ and $(\eta^5\text{-C}_5\text{H}_5)_2\text{Si}$, respectively, it is clear that bent-sandwich molecules feature a total of 14 interstitial electrons (i.e., ring π electrons plus valence electrons from the main-group element).²⁵ When the interstitial electron count exceeds 14 as in, e.g., tetracoordinate group 4A compounds, the cyclopentadienyl rings assume monohapto attachment. Representative examples of this bonding mode include $[(\eta^1\text{-C}_5\text{H}_5)_2\text{SnFe}(\text{CO})_4]_2$ ²⁶ and $(\eta^1\text{-C}_5\text{H}_5)_4\text{M}$ (M = Si, Ge, Sn).²⁷

The 14-electron requirement can be met by using main-group elements other than those from group 4A. For example, cations of group 5A, viz., $[(\text{C}_5\text{H}_5)_2\text{E}]^+$ (E = P, As, Sb, Bi), might be expected to exhibit bis(pentahapto) bonding of the cyclopentadienyl rings.²⁸ To check this idea we have performed an MNDO calculation on $[(\text{C}_5\text{H}_5)_2\text{P}]^+$ (Table IV). One of the

(23) This band is also apparent in the UV PES of Me₅C₅ compounds of the transition metals. Cauletti, C.; Green, J. C.; Kelly, M. R.; Powell, P.; Van Tilborg, J.; Robbins, J.; Smart, J. J. *Electron Spectrosc. Relat. Phenom.* 1980, 19, 327–353.

(24) The ring centroid-heteroatom-ring centroid angles, ν , for the monomeric compounds $(\text{C}_5\text{H}_5)_2\text{Sn}$ (143.7° and 148.0°),¹¹ $(\text{Me}_5\text{C}_5)_2\text{Sn}$ (143.6° and 144.6°),⁵ and $(\text{Me}_5\text{C}_5)_2\text{Pb}$ (151.0°)¹¹ have been determined by single-crystal X-ray diffraction. Since $(\text{C}_5\text{H}_5)_2\text{Pb}$ is polymeric in the solid state,¹⁰ the X-ray value for ν is not very useful for the present purpose. Unfortunately, the electron diffraction value for ν is associated with a large error limit ($135 \pm 15^\circ$).¹⁰

(25) This terminology was employed first by Collins and Schleyer (Collins, J. B.; Schleyer, P. v. R. *Inorg. Chem.* 1977, 16, 152–155).

(26) (a) Bir'yukov, B. P.; Struchkov, Yu. T.; Anisimov, K. N.; Kolobova, N. E.; Skripkin, V. V. *J. Chem. Soc., Chem. Commun.* 1968, 1193–1194. (b) Harrison, P. G.; King, T. J.; Richards, J. A. *J. Chem. Soc., Dalton Trans.* 1975, 2097–2100.

(27) McMaster, A. D.; Stobart, S. R. *Inorg. Chem.* 1980, 19, 1178–1181.

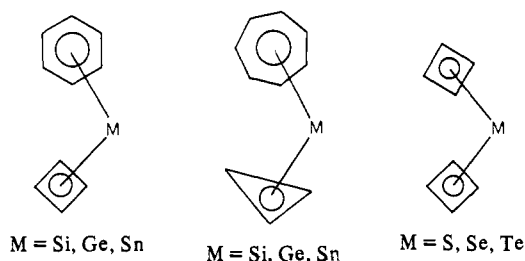
(28) We have recently prepared the arsenium salt $[(\text{Me}_5\text{C}_5)(\text{C}_5\text{H}_5)\text{-As}]^+[\text{AlCl}_4]^-$. NMR evidence suggests that both Me₅C₅ and C₅H₅ rings are bonded in the pentahapto manner. Baxter, S. G.; Cowley, A. H.; Mehrotra, S. K. *J. Am. Chem. Soc.* 1981, 103, 5572–5573.

(29) Rösch, N.; Johnson, K. H. *Chem. Phys. Lett.* 1974, 24, 179–184.

interesting features of this calculation is the fact that, in contrast to the isoelectronic system, $(\eta^5\text{-C}_5\text{H}_5)_2\text{Si}$, the bent-sandwich structure emerges as the ground-state geometry. The strong preference for the C_{2v} rather than D_{5h} (or D_{5d}) bis(pentahapto) structure in the case of the phosphonium ion is a result of the positive charge on the heteroatom and its consequent increased interaction with the cyclopentadienyl rings. In a D_{5h} structure, the HOMO is a degenerate pair of ring π orbitals of symmetry e_1'' . Upon bending to a C_{2v} structure, the e_1'' MO becomes two single degenerate MO's, a_2 and b_2 . Of these the a_2 ring-localized MO is precluded from interaction with P(3s) and P(3p) orbitals for symmetry reasons. The b_2 cyclopentadienyl ring MO can interact with a valence p_y orbital; however, as shown earlier, there is no perceptible interaction between these orbitals in the molecules $(\eta^5\text{-C}_5\text{H}_5)_2\text{Si}$ and $(\eta^5\text{-C}_5\text{H}_5)_2\text{Sn}$. The presence of a formal positive charge on the central atom in the case of $[(\eta^5\text{-C}_5\text{H}_5)_2\text{P}]^+$ increases greatly the interaction between the b_2 ring and P(3p_y) MO's as evidenced by, e.g., the 1.3 eV gap between the 6a₂ and 9b₂ levels (Table IV).

Finally, and more speculatively, we note that bent-sandwich molecules with rings other than cyclopentadienyl might exist. Current efforts are focused on determining whether the 14 in-

terstitial electron rule is applicable in cases such as:



Acknowledgment. The authors are grateful to the Robert A. Welch Foundation and the National Science Foundation (Grant CHE79-10155) for generous financial support. Gratitude is also expressed to Dr. J. F. Nixon of the University of Sussex for the He(II) data.

Registry No. $(\text{Me}_5\text{C}_5)_2\text{Pb}$, 80215-72-1; $(\text{C}_5\text{H}_5)_2\text{Sn}$, 1294-75-3; $(\eta^5\text{-C}_5\text{H}_5)_2\text{Si}$, 81770-35-6; $(\eta^1\text{-C}_5\text{H}_5)_2\text{Si}$, 81790-05-8; $(\text{C}_5\text{H}_5)_2\text{Pb}$, 1294-74-2; $(\text{Me}_2\text{C}_2)_2\text{Sn}$, 68757-81-3; $[(\eta^5\text{-C}_5\text{H}_5)_2\text{P}]^+$, 81770-36-7; $[(\eta^1\text{-C}_5\text{H}_5)_2\text{P}]^+$, 81790-06-9.

pH-Dependent Fluorescence Spectroscopy. 15.¹ Detection of an Unusual Excited-State Species of 3-Hydroxyxanthone[†]

Otto S. Wolfbeis* and Eva Furlinger

Contribution from the Institut für Organische Chemie der Karl Franzens-Universität, A-8010 Graz, Austria. Received November 24, 1981

Abstract: The solvent and acidity dependence of the absorption and fluorescence spectra of 3-hydroxyxanthone and 3-methoxyxanthone has been studied. 3-Hydroxyxanthone is shown to undergo adiabatic photodissociation in aqueous pH 7–2 solution. An unusual species has been detected in the pH 3 to H_0 –2 acidity range, which is characterized by its long-wave emission. This species is assumed to be a phototautomer or an exciplex, formed by proton transfer during the lifetime of the excited singlet state. No evidence for this species is apparent in the UV-absorption spectra. Particular broad-band emissions are found in protic organic solvents together with unexpected effects of acidification. The ground state and first excited singlet state pK_a 's have been determined by either photometry or fluorimetry. The latter were also calculated by applying the Förster–Weller equation. The calculated values do not agree completely with the values obtained by fluorimetry, which may be the result of the noncorrespondence of the ground- and excited-state protolytic equilibria. A ground-state pK_a of 7.16 for 3-hydroxyxanthone together with a fluorescence quantum yield of 0.38 of its anion can make this compound a useful indicator for measuring physiological pH values.

3-Hydroxyxanthone is one of a number of related naturally occurring substances that were isolated from seeds of various plants.^{2,3} It has been extracted from the plant *Kielmeyera excelsa*,⁴ and other 3-hydroxy- and 3-methoxyxanthones are widely distributed in the plant kingdom.⁵ We have focussed our interest on 3-hydroxyxanthone in continuation of our studies on the solvent and acidity dependence of the fluorescence spectra of natural products and because we expected it to be a useful indicator for the fluorimetric determination of physiological pH's.

Experimental Section

Compounds and Solvents. 3-Hydroxyxanthone and 3-methoxyxanthone were prepared according to the procedure given by Ullmann and Wagner.⁶ They were triply recrystallized from ethanol. Stock solutions were prepared in methanol and were diluted with either triple-distilled water or buffer solution to contain finally not more than 10%

methanol. For the measurements in sulfuric acid a stock solution was prepared in concentrated sulfuric acid, which was diluted with triple-distilled water to the desired acidity. H_0 values were taken from Hammett's book.⁷ All solvents were of the best commercially available quality.

Spectra. The absorption spectra were run on a Uvikon 810 spectrophotometer (Kontron, Switzerland, wavelength accuracy ± 0.5 nm, reproducibility ± 0.1 nm) in buffered solutions at room temperature. The fluorescence spectra were recorded on an Aminco SPF 500 spectro-

(1) Part 14. Reference 13.

(2) G. G. De Oliveira, A. A. L. Mesquita, O. R. Gottlieb, and M. T. Magalhaes, *Ang. Acad. Bras. Cienc.*, **38**, 421 (1966); *Chem. Abstr.* **67**, 108528a (1967).

(3) O. R. Gottlieb, A. A. L. Mesquita, G. G. De Oliveira, and M. Teixeira de Melo, *Phytochemistry*, **9**, 2537 (1970).

(4) D. de B. Correa, L. G. Fonseca e Silva, O. R. Gottlieb, and S. J. Goncalves, *Phytochemistry*, **9**, 447 (1970).

(5) F. M. Dean, "Naturally Occurring Oxygen Ring Compounds", Butterworths, London, 1963, Chapter 9.

(6) F. Ullmann and C. Wagner, *Liebigs Ann. Chem.*, **355**, 359 (1907).

(7) L. P. Hammett, "Physical Organic Chemistry", McGraw-Hill, New York, 1970, p 271.

[†]The IUPAC names for 3-hydroxyxanthone (Chemical Abstracts registry No. 3722-51-8) and 3-methoxyxanthone (Chemical Abstracts registry No. 3722-52-9) are 3-hydroxy-9H-xanthen-9-one and 3-methoxy-9H-xanthen-9-one, respectively. The trivial names will be used throughout this paper.